Electronic Supplementary Material (ESI) for Journal of Materials Chemistry A.

Supporting Information for

Stereoassembly of ultrasmall Rh-decorated zeolite imidazolate framework-MXene heterostructures for boosted methanol oxidation reaction

Jinlong Qin,[a] Huajie Huang,*[a] Jian Zhang,[b] Fengyi Zhu,[a] Lang Luo,[a] Chi Zhang,[a] Lu Yang,[a] Quanguo Jiang,[a] Haiyan He*[a]

[a]College of Mechanics and Materials, Hohai University, Nanjing 210098, China

[b]New Energy Technology Engineering Lab of Jiangsu Province, College of Science, Nanjing University of Posts & Telecommunications (NUPT), Nanjing 210023, China

E-mail: huanghuajie@hhu.edu.cn, he.haiyan@hhu.edu.cn

Supplementary Results

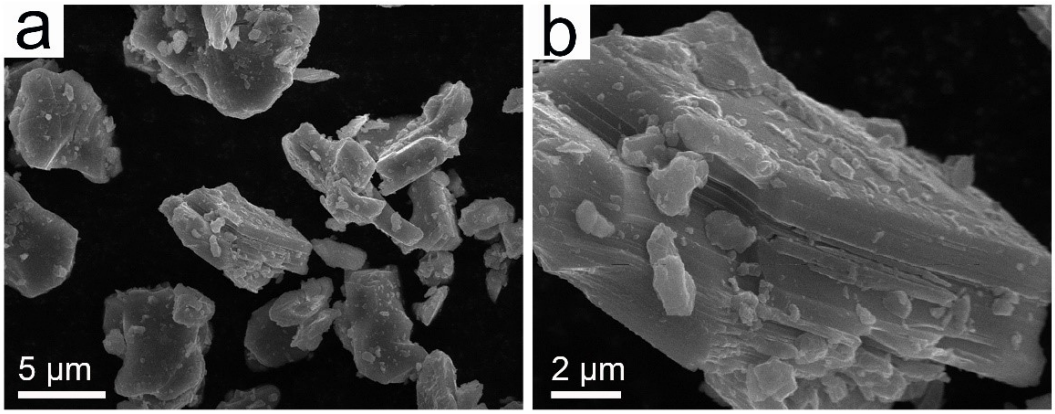

Fig. S1 Representative SEM images of bulk Ti_3AlC_2 at different magnifications.

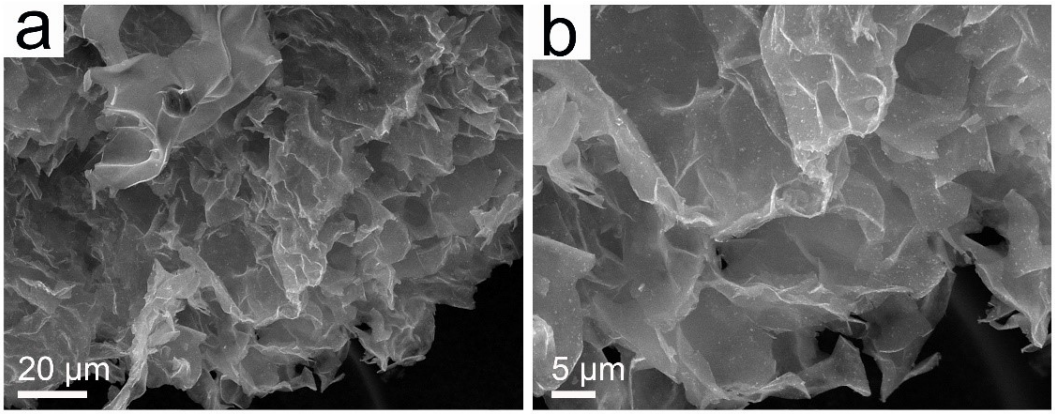

Fig. S2 Representative SEM images of 2D exfoliated $Ti_3C_2T_x$ nanosheets at different magnifications.

Fig. S3 The Tyndall phenomenon of the as-obtained $Ti_3C_2T_x$ MXene solution.

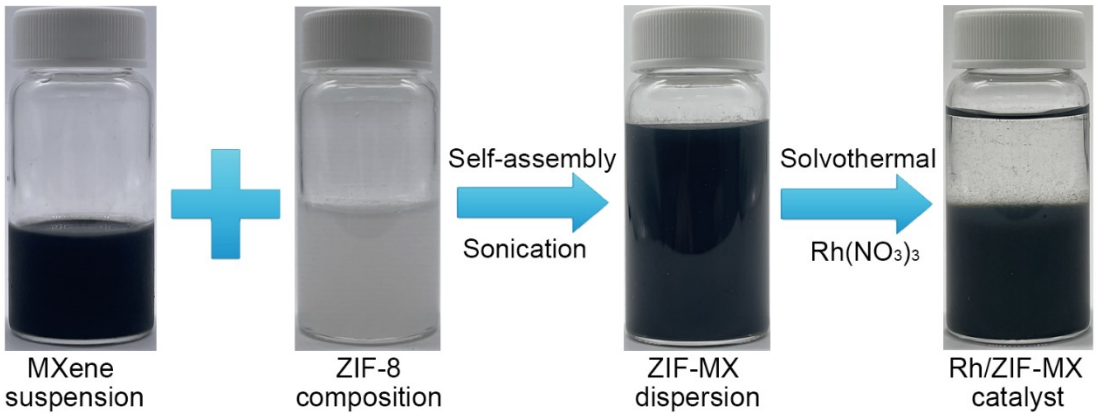

Fig. S4 The synthetic processes for the Rh/ZIF-MX catalyst.

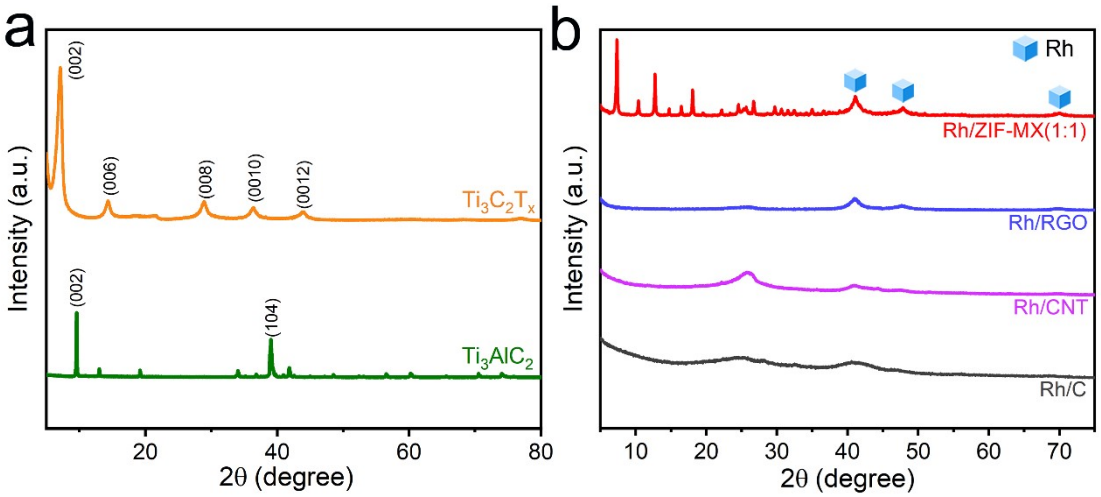

Fig. S5 XRD patterns of (a) the bulk Ti_3AlC_2 and $Ti_3C_2T_x$ nanosheets. (b) XRD patterns of the Rh/ZIF-MX(1:1), Rh/RGO, Rh/CNT and Rh/C samples.

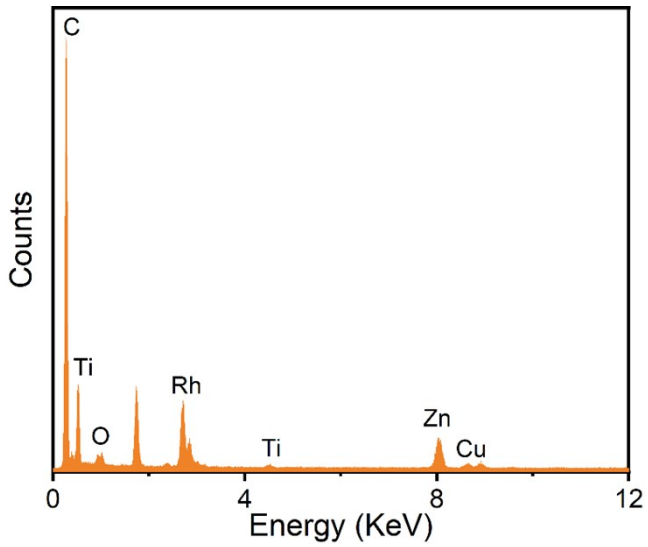

Fig. S6 EDX spectrum of the Rh/ZIF-MX catalyst. The Cu signals were also detected because the sample was held on a Cu grid.

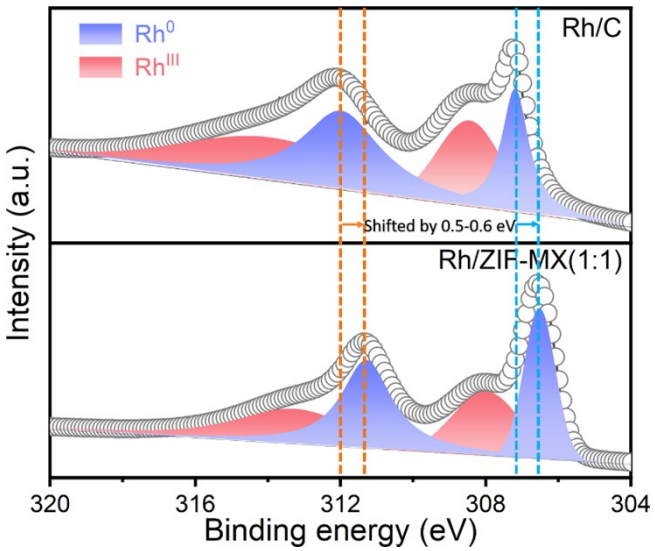

Fig. S7 Comparison of the binding energies for Rh 3*d* spectra of the Rh/ZIF-MX and Rh/C samples.

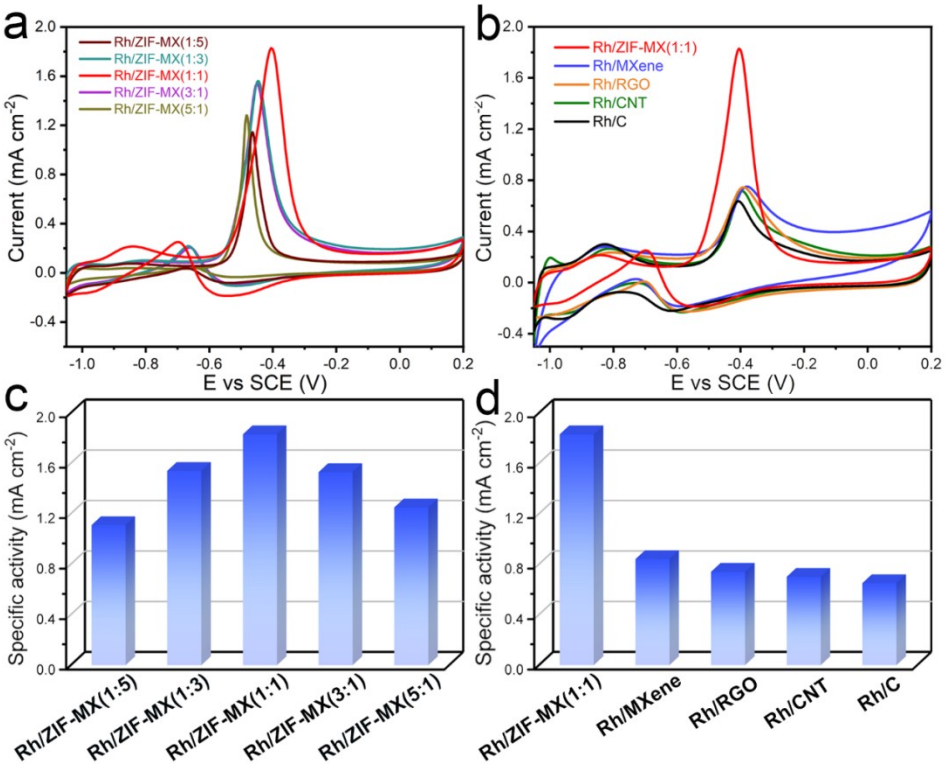

Fig. S8 The ECSA-normalized CV curves of the (a) Rh/ZIF-MX catalysts with different ZIF/MXene ratios and (b) Rh/MXene, Rh/RGO, Rh/CNT and Rh/C in 1 mol L^{-1} KOH with 1 mol L^{-1} CH_3OH solution at 50 mV s^{-1}. (c-d) Specific activities of various catalysts.

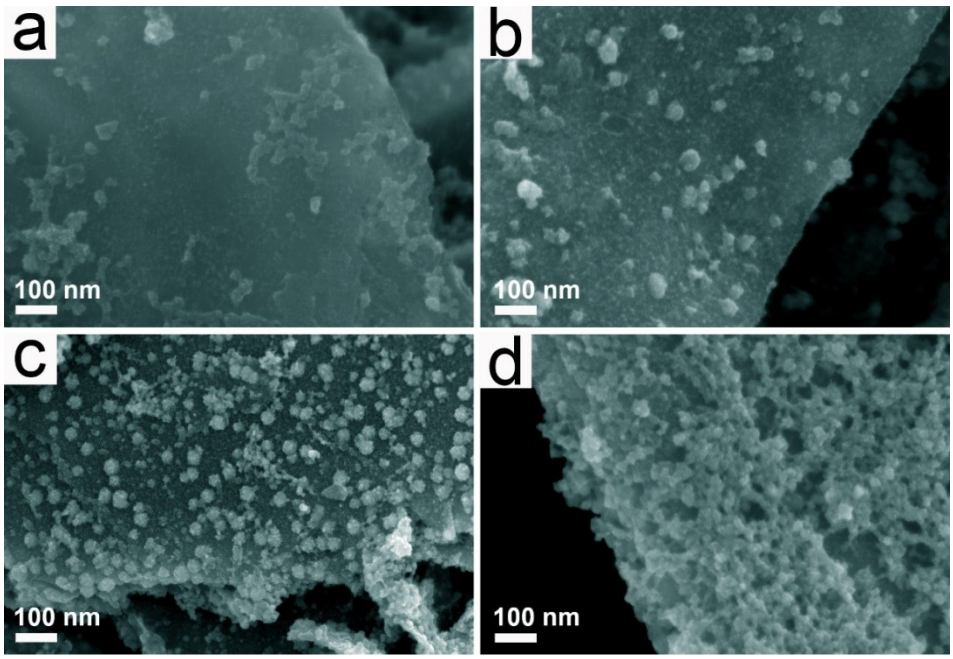

Fig. S9 The FE-SEM images of the (a) Rh/ZIF-MX(1:5), (b) Rh/ZIF-MX(1:3), (c) Rh/ZIF-

MX(3:1) and (d) Rh/ZIF-MX(5:1) samples.

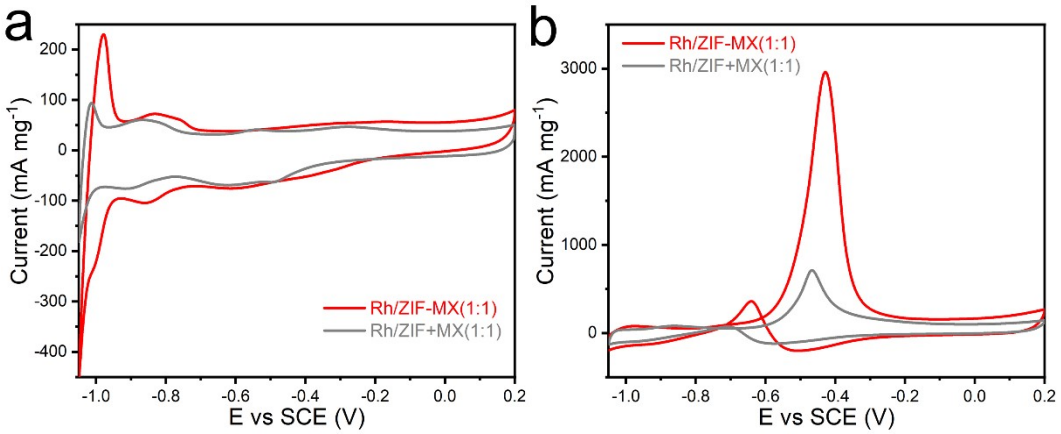

Fig. S10 The CV curves of the Rh/ZIF-MX(1:1) and Rh/ZIF+MX(1:1) electrodes in (a) 1 mol L^{-1} KOH and (b) 1 mol L^{-1} KOH with 1 mol L^{-1} CH_3OH solution at 50 mV s^{-1}.

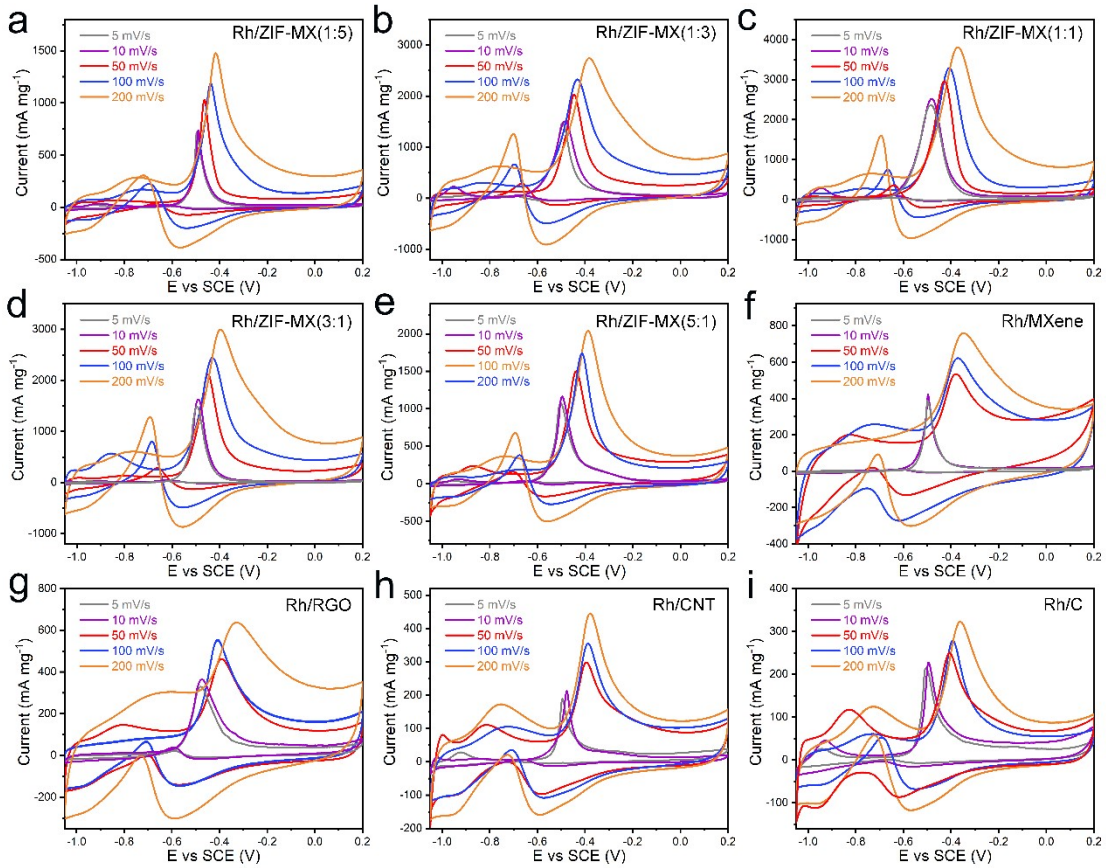

Fig. S11 The CV curves of the (a) Rh/ZIF-MX(1:5), (b) Rh/ZIF-MX(1:3), (c) Rh/ZIF-MX(1:1), (d) Rh/ZIF-MX(3:1), (e) Rh/ZIF-MX(5:1), (f) Rh/MXene, (g) Rh/RGO, (h) Rh/CNT and (i) Rh/C catalysts at different scan rates.

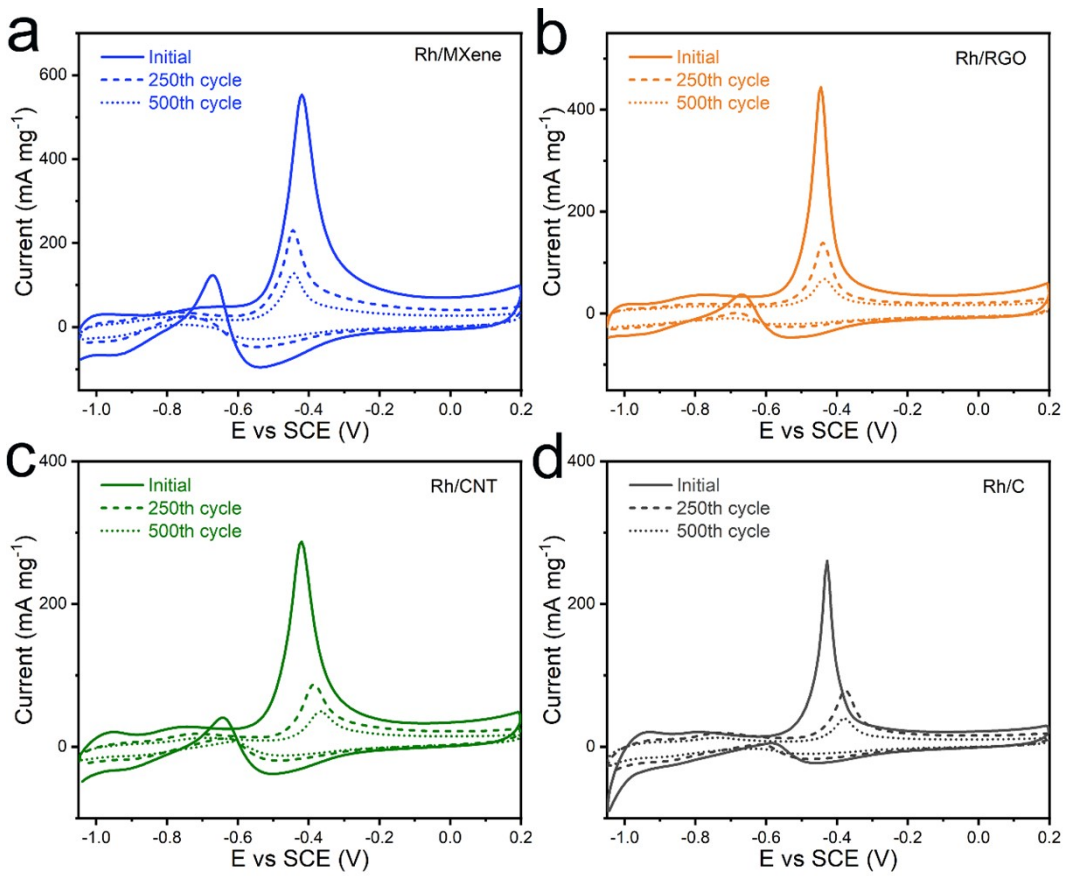

Fig. S12 The CV curves of (a) Rh/MXene, (b) Rh/RGO, (c) Rh/CNT and (d) Rh/C before and after 500 cycles.

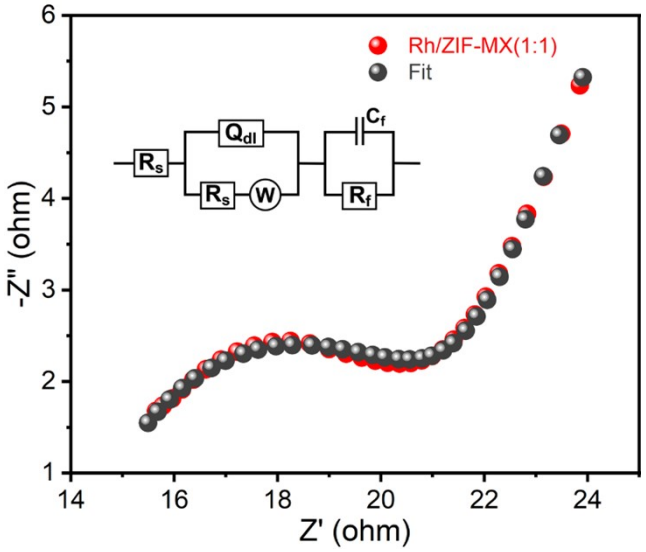

Fig. S13 Nyquist plots of EIS and fitting curve of the Rh/ZIF-MX(1:1) electrode.

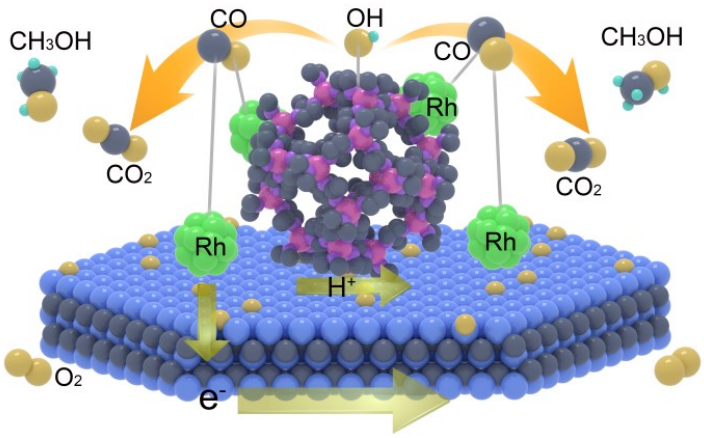

Fig. S14 Schematic diagram of the electrocatalytic processes on the Rh/ZIF-MX electrode.

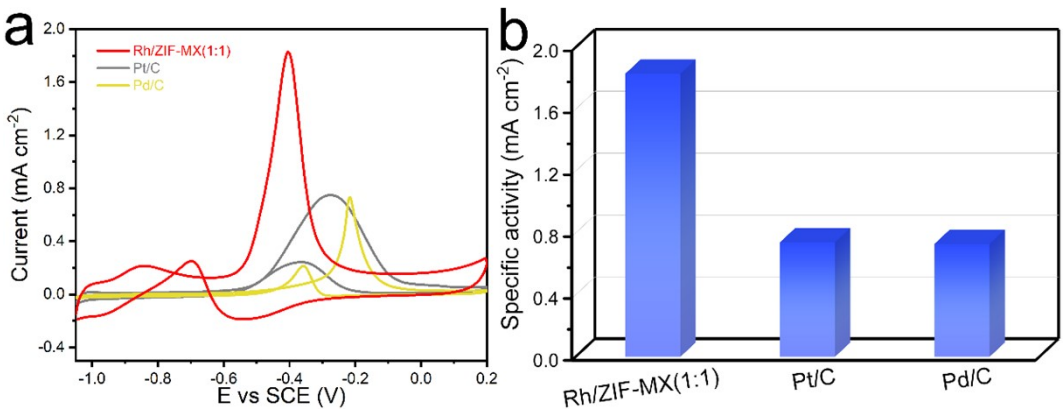

Fig. S15 The ECSA-normalized CV curves of (a) Rh/ZIF-MX(1:1), Pt/C, and Pd/C in 1 mol L^{-1} KOH with 1 mol L^{-1} CH_3OH solution at 50 mV s^{-1}. (b) Specific activities of these three catalysts.

Table S1. Compiled study comparing CV results for different catalysts.

Electrode	ECSA ($m^2\ g^{-1}$)	Mass activity ($mA\ mg^{-1}$)	Specific activity ($mA\ cm^{-2}$)
Rh/ZIF-MX(1:5)	90.2	1000.3	1.11
Rh/ZIF-MX(1:3)	130.1	2000.5	1.54
Rh/ZIF-MX(1:1)	161.5	2955.1	1.83
Rh/ZIF-MX(3:1)	137.8	2109.8	1.53
Rh/ZIF-MX(5:1)	116.4	1450.3	1.25
Rh/MXene	71.2	600.1	0.84
Rh/RGO	62.1	460.6	0.74
Rh/CNT	41.7	293.1	0.70
Rh/C	39.2	255.2	0.65
Pt/C	58.8	425.8	0.72
Pd/C	58.4	430.8	0.74

Table S2. Comparison of methanol oxidation behavior for the Rh/ZIF-MX catalyst and various state-of-the-art Rh-based electrocatalysts.

Catalyst	ECSA ($m^2 g^{-1}$)	Mass activity ($mA mg^{-1}$)	Electrolyte	Ref.
Rh/ZIF-MX	161.5	2955.1	1 mol L^{-1} KOH+ 1 mol L^{-1} CH3OH	This work
Rh/$(MoS_2)_5$-$(RGO)_5$	95.5	1502	1 mol L^{-1} KOH+ 1 mol L^{-1} CH3OH	S1
Rh/CNT-RGO	123.8	1228.5	1 mol L^{-1} KOH+ 1 mol L^{-1} CH3OH	S2
Rh/carbon nanohorns	102.5	784.0	1 mol L^{-1} KOH+ 1 mol L^{-1} CH3OH	S3
Rh/$Ti_3C_2T_x$	71.6	600.0	1 mol L^{-1} KOH+ 1 mol L^{-1} CH3OH	S4
Rh/graphene aerogel	79.6	499	1 mol L^{-1} KOH+ 1 mol L^{-1} CH3OH	S5
Rh nanosheets	73.12	333	1 mol L^{-1} KOH+ 0.5 mol L^{-1} CH3OH	S6
Rh nanotubes	60.9	325	1 mol L^{-1} KOH+ 1 mol L^{-1} CH3OH	S7
Hollow Rh spheres	50.7	292	1 mol L^{-1} KOH+ 1 mol L^{-1} CH3OH	S8
Rh nanosheets/RGO	48.7	264	1 mol L^{-1} KOH+ 1 mol L^{-1} CH3OH	S9
Rh nanodendrites	43.4	255.6	1 mol L^{-1} KOH+ 1 mol L^{-1} CH3OH	S10

Table S3. The charge-transfer resistances (Rct) of different electrodes.

Electrode	R_{ct}	
	Value (ohm)	Error (%)
Rh/ZIF-MX(1:1)	8.1	1.2
Rh/MXene	11.6	1.6
Rh/RGO	23.1	1.9
Rh/CNT	36.8	1.6
Rh/C	4850.0	3.2

Reference

[S1] Q. Zhang, Y. Li, H. He and H. Huang, *ACS Sustainable Chem. Eng.,* 2022, **10**, 8940-8948.

[S2] Y. Li, Y. Chen, J. Qin, J. Chen, Y. Zhao, Y. Xie, H. He and H. Huang, *ChemNanoMat,* 2022, **8**, e202200176.

[S3] X. Guo, Q. Zhang, Y. Li, Y. Chen, L. Yang, H. He, X. Xu and H. Huang, *Rare Met.*, 2022, **41**, 2108–2117.

[S4] J. Qin, H. Huang, Y. Xie, S. Pan, Y. Chen, L. Yang, Q. Jiang and H. He, *Ceram. Int.,* 2022, **48**, 15327-15333.

[S5] Y. Yang, H. Huang, C. Yang and H. He, *ACS Appl. Energy Mater.,* 2021, **4**, 376-383.

[S6] J. Zhu, S. Chen, Q. Xue, F. Li, H. Yao, L. Xu and Y. Chen, *Appl. Catal. B,* 2020, **264**, 118520.

[S7] S. Wang, S. Liu, Z. Wang, Z. Dai, H. Yu, Y. Xu, X. Li, L. Wang and H. Wang, *J. Mater. Chem. A,* 2021, **9**, 4744-4750.

[S8] Y. Kang, Q. Xue, Y. Zhao, X. Li, P. Jin and Y. Chen, *Small*, 2018, **18**, e1801239.

[S9] Y. Kang, Q. Xue, P. Jin, J. Jiang, J. Zeng and Y. Chen, *ACS Sustainable Chem. Eng.,* 2017, **5**, 10156-10162.

[S10] Y. Kang, F. Li, S. Li, P. Jin, J. Zeng, J. Jiang and Y. Chen, *Nano Res.,* 2016, **9**, 3893-3902.